SUPPLEMENTAL INFORMATION

Supplemental Figure 1

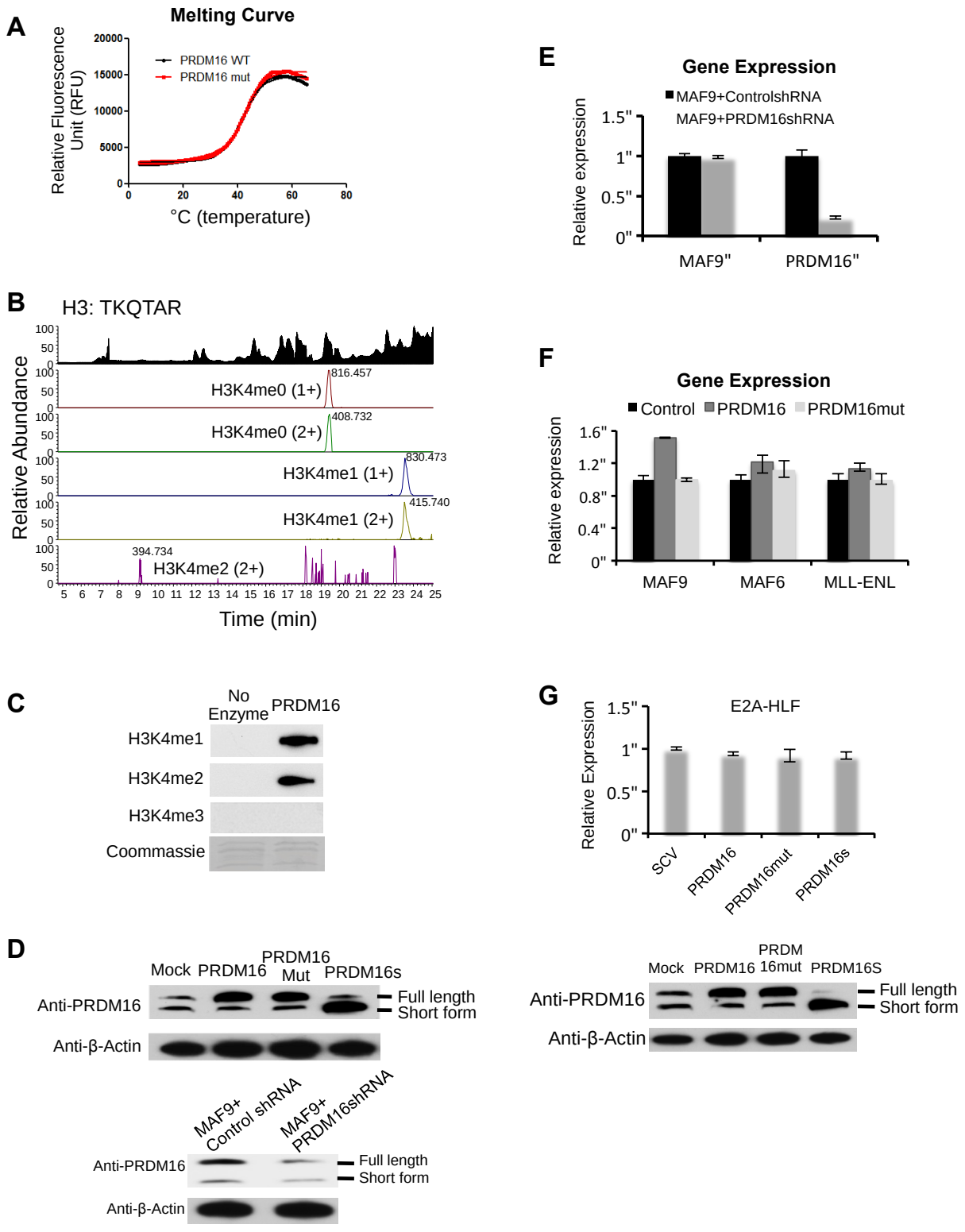

Supplemental Figure 2

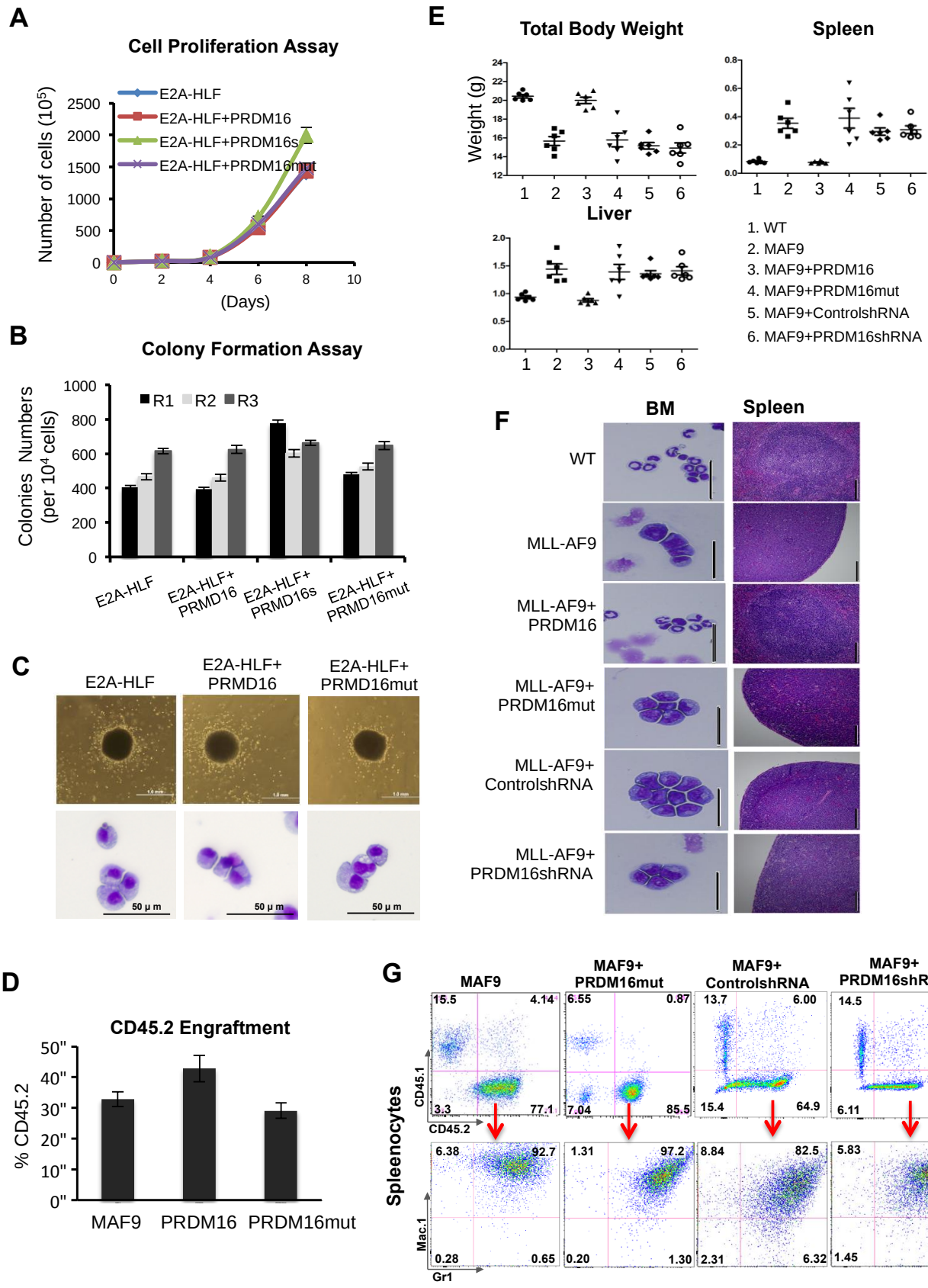

Supplemental Figure 3

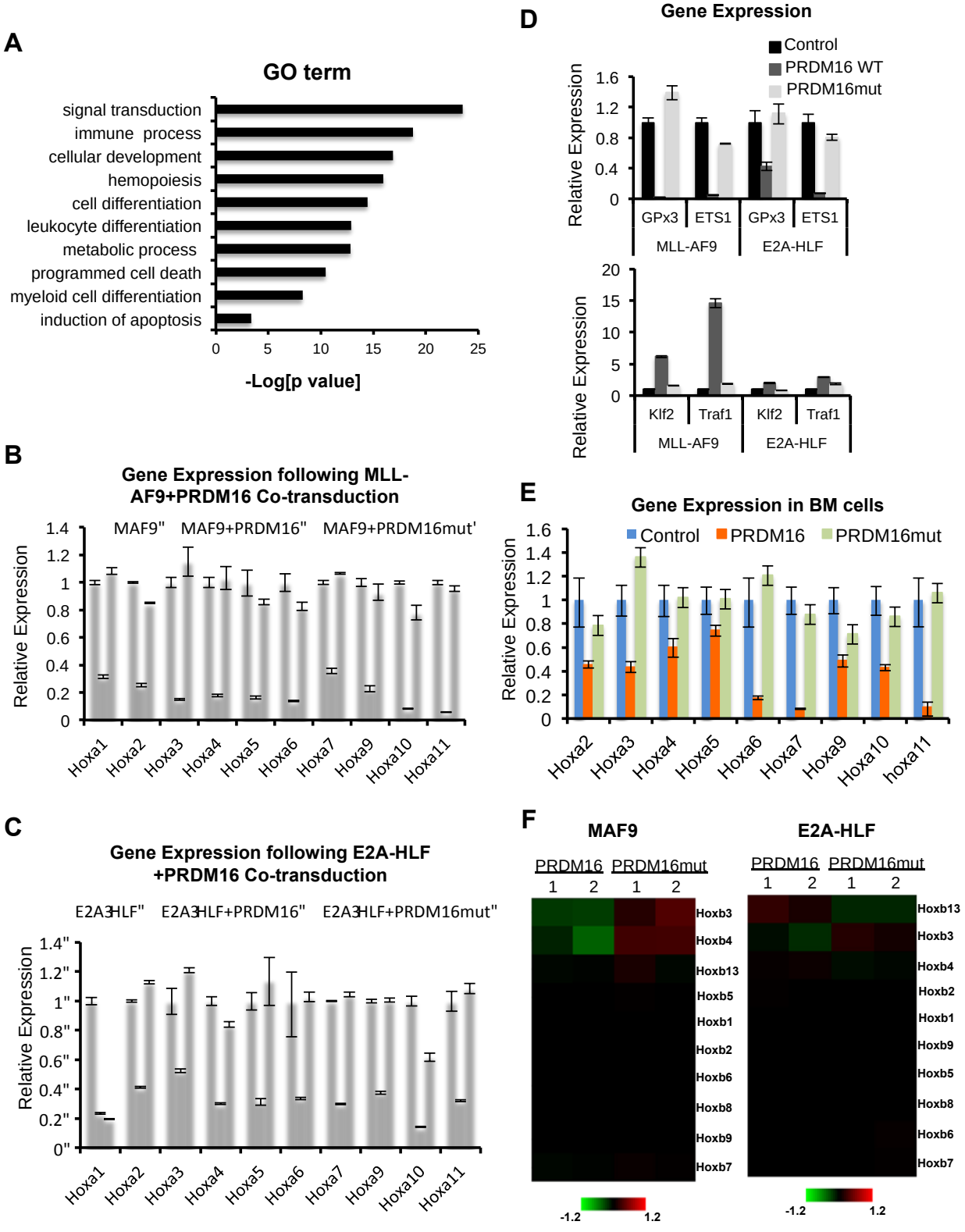

Supplemental Figure 4

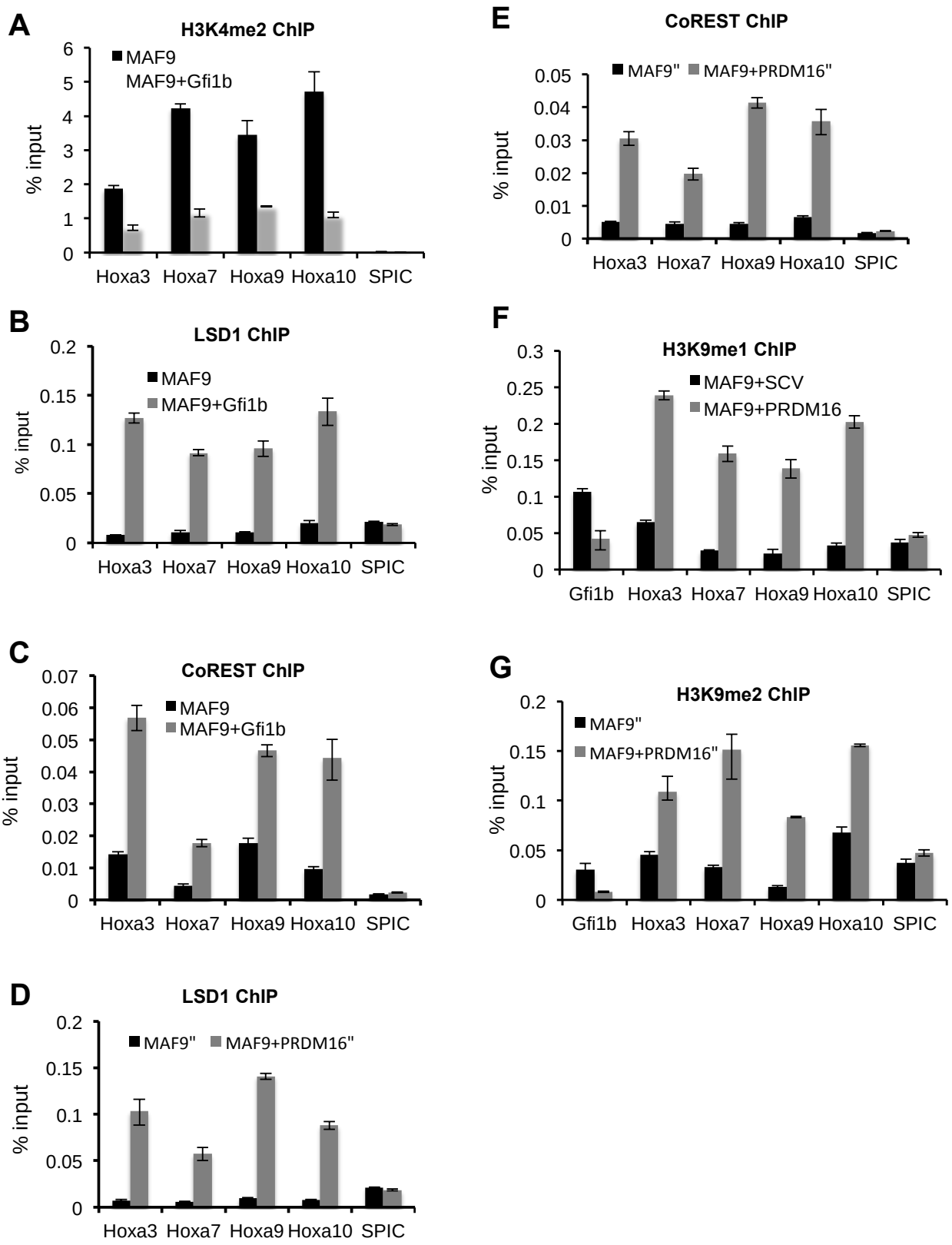

Supplemental Figure 5

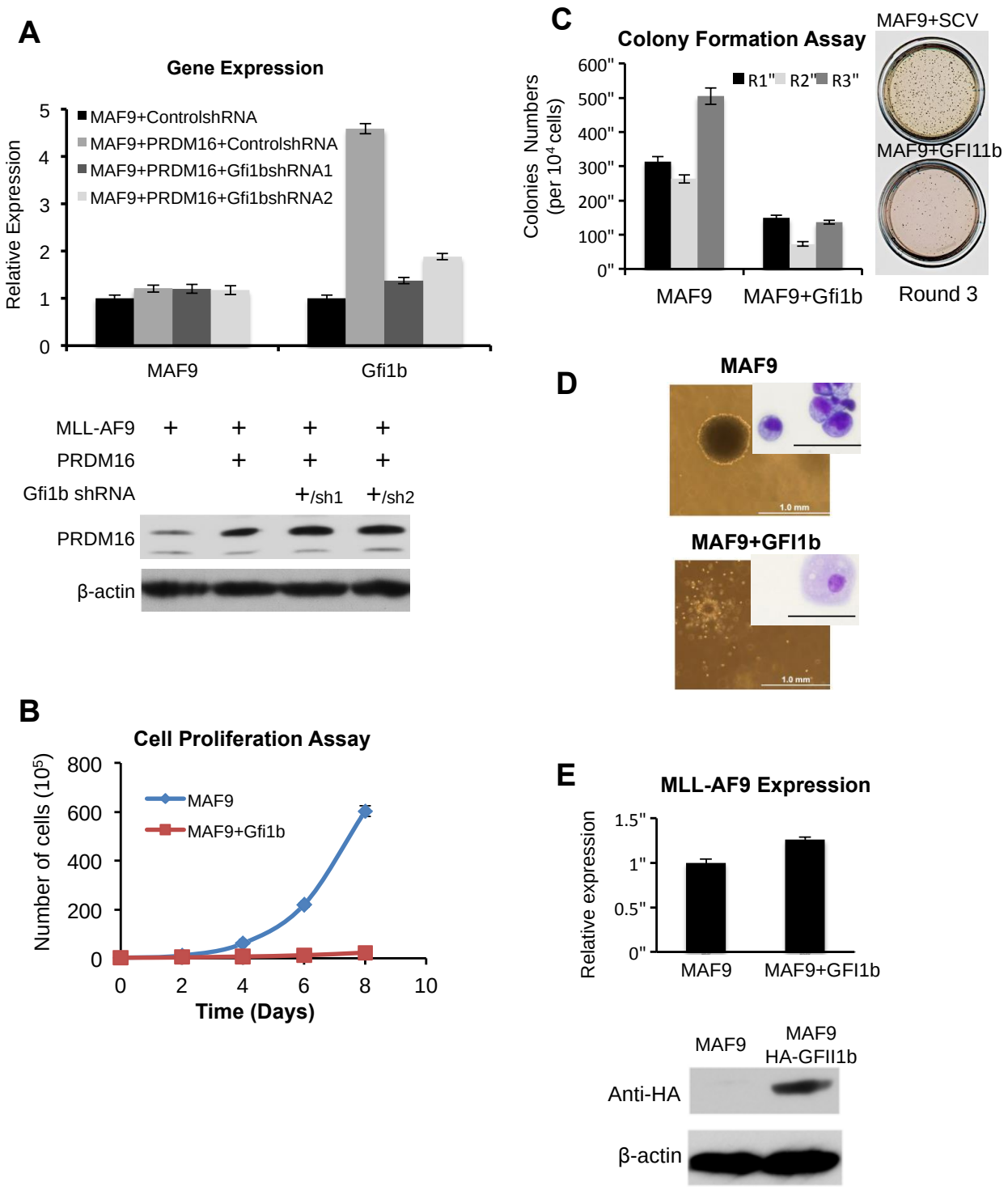

Supplemental Figure 6

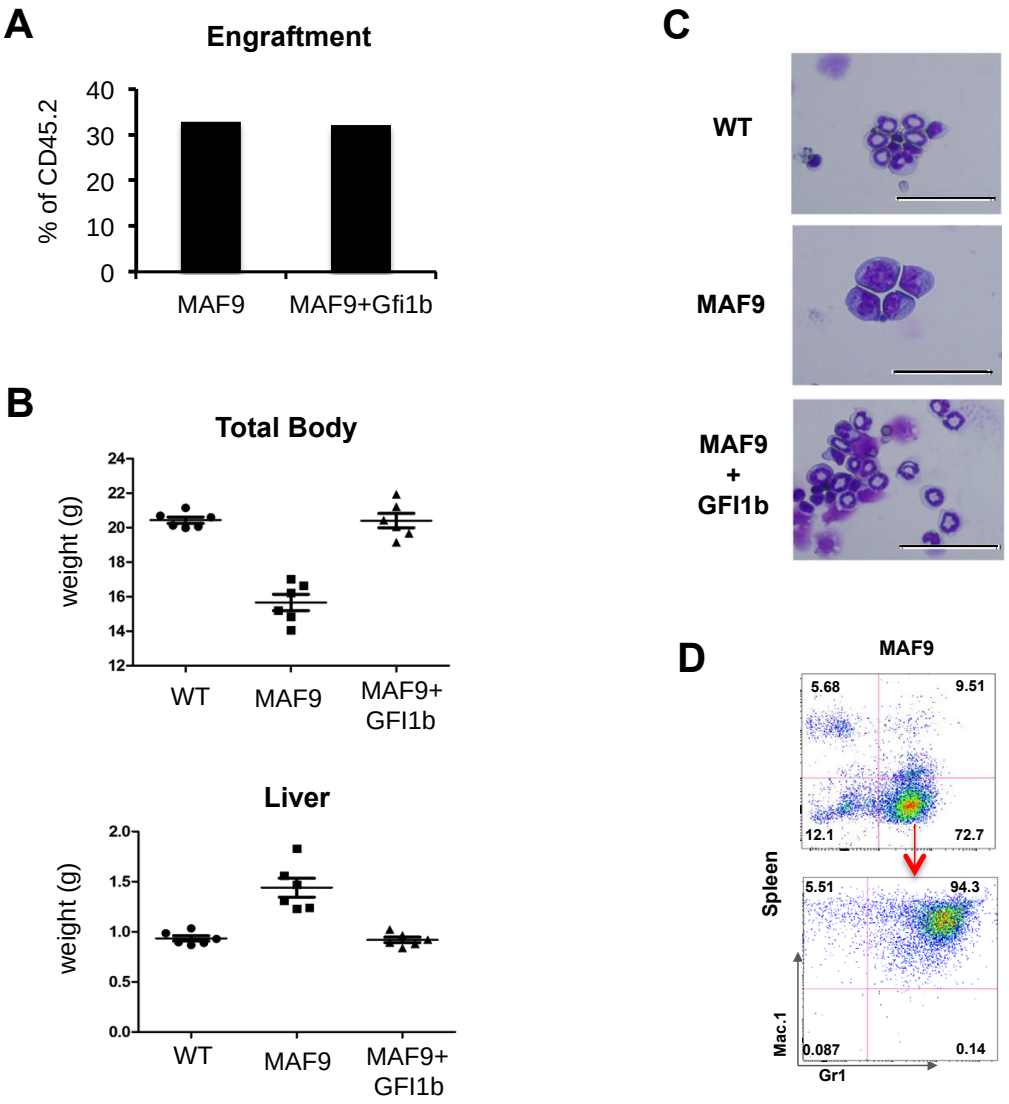

Supplemental Figure 7

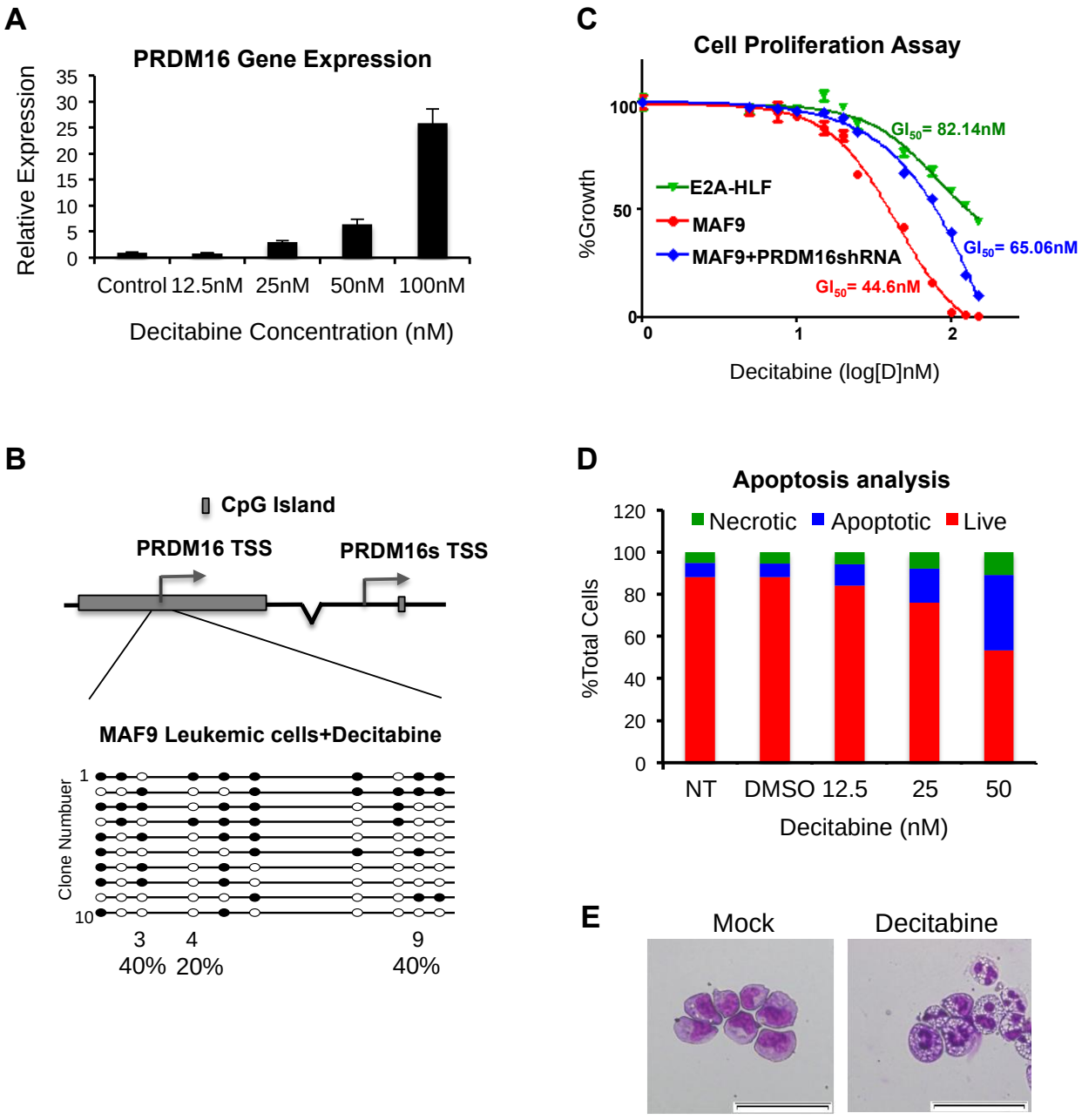

SUPPLEMENTAL FIGURE LEGENDS

Supplemental Figure 1 PRDM16 specifically inhibits MLL-AF9, but not E2A-HLF, leukemia *in vitro.* (This figure is related to Figure1 and 2).

A. Thermal stability comparison of WT and mutant PRDM16. Both proteins were subjected to a temperature gradient in the presence of the fluorescent dye. Melting temperatures were obtained from curve fitting**. B**. LC-MS/MC analysis on PRDM16 methylated nucleosomal H3. Ion chromatograms showed the total ion chromatogram (top) followed by the single ion chromatograms of the trypsin digested H3 TKQTAR peptide after methylation by the wild type PRDM16 enzyme. Parent peaks from the unmodified state (1+ and 2+ charges, at ~19 minutes retention time), the monomethylated state (1+ and 2+ charges, at ~23.8 minutes retention time) and the dimethylated state (2+ charge, at ~9 min retention time) were highlighted. Different apparent mass for H3K4me0/1 vs. H3K4me2 peptides was due to propionlyation of H3K4me0/1, but not H3K4me2, which also affected the retention time of respective peptides (see Supplemental Method). No H3K4me3 or methylation of other lysine residues were detected in the same experiment (data not shown). **C**. Immunoblot for H3 K4 methylation states on nucleosomes after PRDM16 methylation. **D.** Immunoblot for PRDM16 in MLL-AF9 co-transduced cells. Anti-PRDM16 antibody can recognize both PRDM16 and PRDM16S. **E.** Real-time PCR for MLL-AF9 and PRDM16 after treatments as indicated. **F.** Real-time PCR for MLL-AF9, MLL-AF6 and MLL-ENL in *MLL-AF9* or *MLL-AF9* co-transduced cells. **G.** Top showed real-time PCR for *E2A-HLF* expression in different experiments as indicated on X-axis. Bottom showed immunoblots for PRDM16 in *E2A-HLF* cells. Antibodies were indicated on left. For **F** and **G**, gene expression was normalized against *GAPDH* and presented as fold change against oncogene only cells, which was arbitrarily set at 1. Means and standard deviations (as error bars) from at least three independent experiments were presented.

Supplemental Figure 2 PRDM16 suppresses MLL-AF9 leukemogenesis *in vivo*. (This figure is related to Figure 2 and 3).

A. Cell proliferation assay for E2A-HLF after over-expression of PRDM16, PRDM16S and PRDM16mut. Error bars indicated standard deviation (SD) from duplicates. The results were repeated at least three times. **B.** Myeloid colony formation assay. Top, colony counts for primary,

secondary and tertiary plating on methycellulose medium in the presence of IL3, IL6, SCF and GM-CSF. Error bars indicated SD from duplicates. The results were repeated at least three times. Bottom showed representative plates after tertiary plating. **C.** Representative colonies (top) and Wright-Giemas-stained cells (bottom) from the tertiary plating were shown. Scan bar: 50μm. **D.** Engraftment analysis for CD45.2 cells 48-hour post transplantation. Percentage of $CD45.2^{+}$ donor cells against total engrafted cells is shown in each cohort (n=2). **E.** The distribution of the body, spleen and liver weight (g) for recipient cohorts (n=6). Median value and SD (error bars) for each cohort is shown. **F.** Left showed representative Wright-Giemas staining of bone marrow (BM) cells from the recipient mice, scan bar: 50μm. Right showed H&E staining of spleens, scan bar: 200μm. **G.** Flow cytometry analysis of splenocytes for each recipient mice. Top panels: CD45.1 and CD45.2 antibodies. Bottom panels: anti-Mac-1 and Gr-1 antibodies.

Supplemental Figure 3 PRDM16 regulates *Hoxa* gene expression via *Gfi1b*. (This figure is related to Figure 4)

A. Gene ontology (GO) analyses on differentially expressed genes between PRDM16 and PRDM16mut co-transduced *MLL-AF9* cells. **B, C and E.** Real-time PCR for *Hox A* genes in cells as indicated. **D.** Real-time PCR for selective PRDM16 target genes as indicated on bottom. Top panel: genes down-regulated by PRDM16. Bottom panel: genes up regulated by PRDM16. For **B-D**, gene expression was normalized against *GAPDH* and presented as fold change against their respective levels in control cells, which was arbitrarily set at 1. Means and standard deviations (as error bars) from at least three independent experiments are presented. **F.** Heat map for *Hoxb* genes (indicated on right) in *MLL-AF9* and *E2A-HLF* cells as indicated on top. Scale of log2 fold change was indicated on bottom. Duplicate RNA-seq data sets were used.

Supplemental Figure 4 Gfi1b regulates *Hoxa* expression by recruiting LSD1. (This figure is related to Figure 5).

ChIP assay for H3K4me2 (A), LSD1 (B and D), CoREST (C and E), H3K9me1 (F) and H3K9me2 (G) at *Hoxa* genes or *Gfi1b* gene (X-axis). Signals for each experiment were normalized to 1% input. Means and standard deviations (as error bars) from at least three independent experiments were presented.

Supplemental Figure 5 *Gfi1b* overexpression suppresses MLL. (This figure is related to Figure 5).

A. Top, real-time PCR for MLL-AF9 (MAF9) and *Gfi1b* after control or *Gfi1b* shRNA treatment as indicated. Gene expression was normalized against *GAPDH* and presented as fold change against their respective levels in *MLL-AF9+control shRNA* cells, which was arbitrarily set at 1. Bottom, immunoblot for PRDM16 in *MLL-AF9+PRDM16* cells with or without Gfi1b knock down. Immunoblot for β-actin was used as the loading control. **B.** Cell proliferation assay. Cells (Y-axis) were counted every two days (X-axis). Error bars indicate SD from duplicates. The results were repeated at least three times. **C.** Myeloid colony formation assay for MLL-AF9 (MAF9) and Gfi1b co-transduction. Colony counts from three rounds of plating were shown on left. Error bars indicate SD. Representative tertiary plate was shown on the right. The results were repeated at least three times. **D.** Representative images for the tertiary colony (left) and Wright-Giemas-staining of isolated cells (right), scan bar: 50μm. The results were repeated at least three times. **E.** Top shows real-time PCR of MLL-AF9 expression in cells as indicated on bottom. Gene expression was normalized against *GAPDH* and presented as fold change against their respective level in *MLL-AF9* cells, which was arbitrarily set at 1. For **A** and **E**, means and standard deviations (as error bars) from at least three independent experiments were presented. Bottom showed the exogenous HA-GFI1b protein detected by anti-HA antibody.

Supplemental Figure 6 *Gfi1b* overexpression inhibits MLL-AF9 leukemogenesis *in vivo*. (This figure is related to Figure 6).

A. Engraftment analysis for CD45.2 cells 48-hour post-transplantation. **B.** The distribution of total body weight (top) and the liver weight (bottom) for each cohort (n=6). **C.** Representative Wright-Giemas staining of bone marrow (BM) cells from each cohort as indicated on top. Scan bar: 50μm. For **B**, median value and SD (error bars) for each cohort were shown. **D.** Flow cytometry analysis of splenocytes. Antibodies used for staining: top panels: anti-CD45.1 and CD45.2; bottom panels: anti-Mac-1 and Gr-1.

Supplemental Figure 7 PRDM16 is regulated by DNA methylation. (This figure is related to

Figure 7).

A. Real-time PCR for *PRDM16* 72-hour after Decitabine treatment at various concentrations as indicated on bottom. Gene expression was normalized against *GAPDH* and presented as fold change against their respective level in mock treated cells, which is arbitrarily set at 1. Means and standard deviations (as error bars) from at least three independent experiments were presented. **B.** Bisulfite-sequencing results for 10 clones from experiments using MLL-AF9 leukemic cells 72-hours after Decitabine treatment, which was similar to experiments shown in Figure 7. Percentage of methylated individual CpG site was indicated on bottom. **C.** Cell proliferation assay for *MLL-AF9, E2A-HLF* and *MLL-AF9+PRDM16shRNA* cells by CellTiter-Glo. Cell growth was presented as percentage of mock-treated cells. Means and SD from three experiments were presented. IC50s were shown. **D.** Apoptotic assay was performed for MLL-AF9 cells 48-hours after Decitabine treatment at various concentrations (X-axis). Numbers of apoptotic, necrotic and live cells were presented as percentage of non-treated cells (Y-axis). **E.** Wright-Giemsa staining of *MLL-AF9* cells 72-hours after mock or Decitabine (50nM) treatment. The most representative cells were selected for imaging.

SUPPLEMENTAL TABLES

Supplemental Table S1 Complete list of genes that show 2-fold difference in expression between MLL-AF9/PRDM16 and MLL-AF9/PRDM16mut co-transduced cells. This table is related to Figure 4.

Supplemental Table S2 Complete list of GO analyses for biological pathways of genes that are regulated by PRDM16 activity. This table is related to Figure 4.

Supplemental Table S3 Complete list of genes that show > 2-fold differences in expression between PRDM16 and PRDM16mut in both MLL-AF9 and E2A-HLF cells co-transduced cells. This table is related to Figure 4.

Supplemental Table S4 Complete list for the primers used in real-time PCR experiments. This table is related to Figure 4, 5 and 6 and Supplemental Figure 1, 3, 4 and 7.

Supplemental Table S2 GO analyses for PRDM16 activity dependent gene pathways in MLL-AF9 co-transduced cells.

GO_ID	Term	p_value	FDR	Enriched (FDR<0.05)
GO:0009966	signal transduction	3.26E-24	1.98E-21	YES
GO:0002684	immune process	1.82E-19	5.61E-17	YES
GO:0048869	cellular development	1.39E-17	3.26E-15	YES
GO:0030097	hemopoiesis	1.09E-16	2.23E-14	YES
GO:0045595	cell differentiation	3.57E-15	5.79E-13	YES
GO:0002521	leukocyte differentiation	1.28E-13	1.74E-11	YES
GO:0012501	programmed cell death	3.50E-11	3.56E-09	YES
GO:0030099	myeloid cell differentiation	5.70E-09	4.19E-07	YES
GO:0006917	induction of apoptosis	0.0004059	0.007937	YES

Supplemental Table S4 Primers used for clone and real-time PCR confirmation

Name	Forward	Reverse
PRDM16-Hta	GCCGCGAATTCGATCCAAGGCGAGGGCGAGG	GCGCTCGAGTAAGATGCCCGGGAAGCCGG
PRMD16mut	AGGCTGGGCCCCTTCGTGGCGGTGCCCCGG	CGCCCGGGGCACCGCCACGAAGGGGCCCAG
PRDM3-Hta	CGCGAATTCATGAAGAGCGAAGACTATCCC	GCGCTCGAGTTAGGGCCTCTCTTCAGAGGACCT
PRMD3mut	GAAGTAGGTGAAAAGTTTGGGCCTGAGCAGAGGTCAAACCTGAA	GTCTTTCAGGTTTGACCTCTGCTCAGGCCCAAACTTTTCACCTA
Mouse Prdm16mut	TCGGGGAGAGGTTTGGCCCCTTCGTGGCGACGCCCCGGGCCGCACT	CTTCAGTGCGGCCCGGGGCGTCGCCACGAAGGGGCCAAACCTCTCC
Prdm16S-SCV	GCGCTCGAGATGTACCCATACGATGTTCCAGATTACGCTATGTGTCAGATCAACGAACAG	CGCGAATTCTCAGAGGTGGTTGATGGGGTTAAAGG
Prdm16fullrt	GAGATGCTGACGGATACA	CTCGCTACCCAAGTCTTC
PrdmSrt	ATATGCGGAGAAGGTCAA	CGGTCGTGGTGTTGATAT
Gfi1b-SCV	GCGCTCGAGATGTACCCATACGATGTTCCAGATTACGCTCCACGGTCCTTTCTAGTGAAGAGTAAGAAGGCA	CGCGAATTCTCACTTGAGATTGTGTTGACTCTCACGGTG
Gfi1brt	AAGAGCATAGCCAGAGTG	TGATTGTGTTCCAGTCCAA
Hoxa1rt	AAACAGGGAAAGTTGGAGAG	GCTGCTTGGTGGTGAAAT
Hoxa2rt	TTCCCAGTTTCGCCTTTA	TGTTGACAAGCAGTTAGGA
Hoxa3rt	AAGCGACCTACTACGACAG	TGGCATTGTAAGCGAACC
Hoxa4rt	CAGAACCGGAGAATGAAGTG	CGAGGCAGTGTTGGAAGA
Hoxa5rt	TTCCACTTCAACCGCTAC	TTCCACTTCATCCTCCTG
Hoxa6rt	TTACCAACAGTCCAACTC	GGTCTTTATCAGAATAGAAACA
Hoxa7rt	TCTTCGTATTATGTGAAC	CTGTTGACATTGTATAAG
Hoxa9rt	GGTTCTCCTCCAGTTGATAG	GCTCTCATTCTCGGCATT
Hoxa10rt	CCTAGAGATCAGCCGTAG	AGTTTCATCCTGCGATTC
Hoxa11rt	TTCTTCTTCAGCGTCTAC	TTCCTTCATTCTTCTGTTCT
Hoxa13rt	GGGAATACGCTACGAACA	GATTGTGACCTGCCTCTC
Hoxa1TSS chip	CCTGCCCACTAGGAAGCGGTC	CAGGGCTTCGCAGGATCCAAT
Hoxa2TSS chip	CAAATTCGTAATTCATGGCCT	CCATACGGCTGTAATCAGTGA
Hoxa3TSS chip	CCTACAAAGACCGGGATGGGA	GGCTAGGCCCAACCCTGTTAG
Hoxa7TSS chip	AACCCTTCCCCTAAACGCCTC	AAAAGGTCGCCAGTCTTCCAG
Hoxa9TSS chip	ATCTGTATGCCTAGTCCCGCTCC	TTGATGTTGACTGGCGATTTTC
Hoxa10TSS chip	CTGGCTCTTGAACCTGTACCCC	CAAGGGTGCTTCCAAATAGTC
Gfi1bTSS chip	CGCCAGATTTTGACACAA	CAGACAGACACTTCTCCTT
Hoxa3Gfi1bbinding chip	TTAGCTTCGGCACACTGT	AACCATCGGAGAACTCTGAAT
Hoxa7Gfi1bbinding chip	TTGGCATTCTACTGTTCC	ACTACCTCTGGCTATTGG

Hoxa9Gfi1bbinding chip	TTCCATCTTTCTGTCCAAATC	TCTAAGCCAGCCCTTTAC
PRDM16 BSP	GGTTTGGGTAGGAGTTATAG	CTAACCCTTTAAAAAAACATTCCTTACT
GPx3	CCAGTCTCAAGTATGTTC	GTTCTTCAGGAAAGTGTA
ETS1	TTACACCTCGGATTACTT	ATAGGACTCTGTGATGAA
Klf2	GGCAAGACCTACACCAAG	GCAATGATAAGGCTTCTCAC
Traf1	ACTCAGGAGAAGGTTCACT	TGAAGGAACAGCCAACAC

SUPPLEMENTAL METHODS

Preparation of Histones, recombinant nucleosome and BM cells histones extraction.

Recombinant Nucleosomes were constituted by salt dialysis. 146bp DNA fragment containing 601 sequence was mixed with recombinant histone octamer in high-salt buffer (20mM Tris-HCl, 2.5M NaCl, 0.5mM EDTA, and 1mM DTT). The mixture was dialyzed at 4°C against gradual change to low-salt buffer (20mM Tris-HCl, 50 mM NaCl, 0.5mM EDTA, and 1mM DTT) at a rate of 0.8ml/min. The nucleosomes were further purified by preparative PAGE gel. The purified recombinant nucleosomes could be visualized on 4.5% native gel after ethidium bromide staining. For isolating histones from cells, 2~3X10^6 cells were collected and histones were extracted using the HCl acid described in previous publication (Shechter et al., 2007).

In vitro HMT assay

For each HMT assay, 0.5μg recombinant enzymes, 2 μg free Histones or 2μg recombinant nucleosomes were used. Reactions were carried out at 30°C for 1 hour in the presence of 10μM H^3-SAM with HMT buffer (20mM Tris-HCl [pH 7.8], 5mM DTT, 0.5mM EDTA and 10% glycerol). The methylation was detected by autoradiograph.

Thermo shift assay

To compare thermal stability of WT and mutant PRDM16, a thermal shift assay was performed in the presence of Protein Thermal Shift Dye (ThermoFisher), following the manufacturer's protocol. In brief, the Protein Thermal Shift Dye was first diluted to 8X working solution prior to adding to the samples. Next, 3μg of protein (WT or mutant PRDM16) or equivalent volume of buffer was mixed together with 5μL of Protein Thermal Shift buffer, 12.5μL of the diluted 8X dye in a Bio-Rad 96-well hard-shell microplate on ice. Final reaction volume was 20μL for all samples and set in triplicate. Fluorescent melt curves were obtained on a Bio-Rad CXF-96 real-time PCR machine under FRET mode, with the following temperature steps: (1) 4ºC for 10 minutes, and the microplate was placed in the instrument once heating block reached 4ºC (2) a temperature gradient going from 4ºC to 85ºC at 0.5ºC per cycle and 1-minute incubation per degree increment (3) acquired fluorescence reading at each cycle. Fluorescence melt curves were fitted for melting temperature calculations in GraphPad Prism using Boltzmann Sigmoidal model after

manual baseline subtraction.

Mass Spectrometry

Recombinant nucleosomes modified by PRDM16 were chemically derivatized using propionic anhydride and digested to peptides with trypsin, followed by another round of derivatization as described previously (Bhanu et al., 2015). Peptides desalted using C_{18} stage-tips were analyzed using an EASY-nLC nanoHPLC (Thermo Scientific, Odense, Denmark) coupled with a Q-Exactive mass spectrometer (Thermo Fisher Scientific, Bremen, Germany). HPLC gradients and mass spectrometry parameters are defined previously (Bhanu et al., 2015). The MS/MS events targeted the H3K4 unmodified, mono, di and trimethyl peptides to enable quantification of even low abundant marks.

Cell Proliferation, Cell Viability and Apoptosis

For cell proliferation assay, transduced cells were selected by 1mg/ml G418 and 1.5 ug/ml for 10 days. The starting cell density is ~$1X10^5$/ml and the cells were counted every two days.

Cell viability assay was performed as described previously (Cao et al., 2014). Cells were treated with Decitabine (Abcam) at various concentrations for 3 days. 0.05%DMSO was used as the control. Viability was determined using the CellTiter-Glo Kit (Promega) according to the manufacture's protocol. For apoptosis assay, MLL-AF9 leukemia cells were seeded at the concentration $1X10^4$/ml. They were treated with Decitabine or DMSO for 2 days before harvest. The cells were washed and suspended in 1X Anenexin V binding buffer (BD Pharmingen) with APC-conjugated Annexin V (BD Pharmingen) and prodidium iodide (PI) for 15 minutes and subject to flow cytometry analyses.

The GFI1b immunoprecipitation

$6X10^8$ BM cell co-transduced with MLL-AF9 and HA-Gfi1b were collected. The cells were lysed in buffer (20mM Tris-HCl pH7.5, 300mM NaCl, 0.2%NP40 and 1mM PMSF) on ice for 30min and then subject to 1min sonication (10% output). Whole cell lysate was incubated with anti-HA Affinity gel (Sigma E6779) at 4°C for 4 hours and then washed with lysis buffer 5 times. The bound proteins were eluted by buffer containing 8M Urea,

0.4M ammonium bicarbonate and 1% SDS. The eluted sample was resolved by SDS-PAGE and blotted by specific antibodies.

Antibody Information

All antibodies are available from commercial sources. They include: H3K4me1 (07-450), H3K4me2 (07-030), H3K4me3 (07-473), H3K27me3 (07-449) (Millipore). H3K9me2 (Abcam ab1220), LSD1 (Abcam ab17721), HA (Abcam ab9110), CD45.1-PE (Biolegend 110708), CD45.2 (Biolegend 109828), Mac1-PE (eBioscience 9012-0118-120), Gr1-APC (eBioscience 17-5931-82), CD3-PE (Biolegend 1000206), CD19-APC (eBioscience 17-0193-82), 5-Methylcytosine (Eurogentec, BI-MECY-0500), dynabeads® M-280 Sheep Anti-Mouse IgG (Thermo Fisher Scientific, 11201D), H3K9me1 (Abcam ab9045), MED1 (Millipore 17-10530), PGC-1α (Millipore ST1202) and CoREST (Millipore 07-455).

RNA-seq data analyses

Sequenced reads were aligned to mouse reference genome (mm9) using Bowtie and Tophat (version 2.0.3) (Langmead et al., 2009; Trapnell et al., 2009). The program Cuffdiff was used for differential gene expression analysis (Trapnell et al., 2010). Genes with expression fold change >=2 and FDR <= 0.05 were defined as significant. Gene set enrichment analysis (GSEA, http://www.broadinstitute.org/gsea/index.jsp) was performed on gene expression of PRDM16 versus PRDM16 mutant co-transduced cells. Gene ontology (GO) analysis was performed on the 2751 differentially expressed genes using GOseq (Young et al., 2010). Heatmap was made using cantered expression values with Cluster 3.0 and TreeView (http://jtreeview.sourceforge.net/). Scatter plot for gene expression analyses was performed using Gnuplot software.

SUPPLEMENTAL REFERENCE

Cao, F., Townsend, E.C., Karatas, H., Xu, J., Li, L., Lee, S., Liu, L., Chen, Y., Ouillette, P., Zhu, J., *et al.* (2014). Targeting MLL1 H3K4 methyltransferase activity in mixed-lineage leukemia. Mol Cell *53*, 247-261.

Bhanu NV, Sidoli S, Garcia BA. Histone modification profiling reveals differential signatures associated with human embryonic stem cell self-renewal and differentiation. Proteomics. 2015 Dec 3. [Epub ahead of print]

Shechter, D., Dormann, H.L., Allis, C.D., and Hake, S.B. (2007). Extraction, purification and analysis of histones. Nature protocols *2*, 1445-1457.

Langmead, B., Trapnell, C., Pop, M., and Salzberg, S.L. (2009). Ultrafast and memory-efficient alignment of short DNA sequences to the human genome. Genome Biol 10, R25.

Trapnell, C., Pachter, L., and Salzberg, S.L. (2009). TopHat: discovering splice junctions with RNA-Seq. Bioinformatics 25, 1105-1111.

Trapnell, C., Williams, B.A., Pertea, G., Mortazavi, A., Kwan, G., van Baren, M.J., Salzberg, S.L., Wold, B.J., and Pachter, L. (2010). Transcript assembly and quantification by RNA-Seq reveals unannotated transcripts and isoform switching during cell differentiation. Nat Biotechnol 28, 511-515.

Young, M.D., Wakefield, M.J., Smyth, G.K., and Oshlack, A. (2010). Gene ontology analysis for RNA-seq: accounting for selection bias. Genome Biol *11*, R14.